The effect of dimple and perforations on Flow Efficiency and heat transfer enhancement in Multi louvered Fin banks

Dr. H. Shokuhmand [1], F.Sangtarash [2]

[1.] Professor of Mechanical Engineering, Department of Mechanical Engineering, University of Tehran, Tehran, Iran
hshkuhmand@me.ut.ac.ir
[2.] P.H.D Student , Department of Mechanical Engineering, University of Tehran, Tehran, Iran
fsangtarash@me.ut.ac.ir

Abstract: Numerical and experimental analyses are performed on multi-louvered fin banks in low and medium Reynolds regimes to investigate the effects of dimples and perforations on flow structure and heat transfer capacity. In different Reynolds numbers the flow efficiency has been calculated numerically and experimentally by flow visualization method and the results show that dimple and perforations can increase flow efficiency more than 5% in fin banks. In addition to flow efficiency evaluation a set of numerical and experimental analysis has been done to evaluate temperature contours and total heat transfer in three cases of simple fin bank, dimple fin bank and dimple-perforation fin bank in different Reynolds Numbers. The results show that employing dimples and perforations together because of using heat transfer enhancement features of non-continuous surfaces with those of interrupted surfaces leads to considerable raise in heat transfer capacity of the fin banks up to 9% in fin banks.
[Shokuhmand, F. Sangtarash. **The effect of dimple and perforations on Flow Efficiency and heat transfer enhancement in Multi louvered Fin banks.** *Life Sci J* 2013;10(9s):30-40] (ISSN:1097-8135). http://www.lifesciencesite.com. 4

Keywords: multi-louvered fin, dimple, flow efficiency, perforation, heat transfer enhancement

Introduction

Widespread application of compact heat exchangers in automotive, HVAC and refrigeration industries has necessitated the use of various ways to augment the air side heat transfer capacity. Interrupted surface is a way to enhance the heat transfer by reforming the thermal boundary layer. One of the most widely used designs among interrupted surfaces is the multilouvered geometry. During past decades many experimental and numerical studies have been conducted to demonstrate the flow characteristics [1-7].

Beauvias [2] was the first to perform flow visualization experiments on the louvered fin array. He showed that rather louvers actually acted as guides to redirect the flow in between them. Flow visualization performed by Davenport [3] demonstrated two asymptotic flow regimes; duct directed flow, and louver directed flow. In the former the predominant flow is stream wise while in the latter the predominant flow is aligned with the louvers. Zhang and Tafti [4] showed that the flow direction has significant implications on the overall heat capacity of the fin because of its strong effect on the heat transfer coefficient. Therefore it is important to be able to quantify the flow regime. In order to do so a parameter called “flow efficiency” is defined as the degree to which the flow is aligned to the louver direction [3-5]. A 100% efficiency represents complete louver directed flow while 0% represents complete duct flow [4].

The importance of predominant flow directions was soon discovered in early multilouver studies [2-5]. Zhang and Tafti [6] showed that high flow efficiency enhances the heat transfer coefficient. Flow efficiency in general, is a function of Reynolds number and geometrical parameters like fin pitch, louver angle and louver thickness ratio [4,6]. Consequently a critical Reynolds number, after which the flow efficiency is independent of the louver angle, was identified [4].

Achaichia et al studied the flow pattern along with k-epsilon turbulent model for high Reynolds numbers [8]. However, high Reynolds turbulent models are not very accurate in unsteady laminar and low Reynolds number turbulence regimes encountered in compact heat exchangers.

Zhang et. al [9-10] and Tafti et al [11-12] have studied the effects of flow oscillations in the form of large-scale vorticity on the heat transfer coefficient. Tafti [12] investigated the transition from steady laminar to unsteady flow in a multilouvered fin array. The local heat transfer from the fin surface was found to be strongly affected by the large-scale vortices shed from the louver.

Zhang and Tafti studied the effects of Intra-fin and Inter-fin thermal wakes on the heat transfer capacity of the fin array. They suggested that thermal wake effects can be expressed as functions of the flow efficiency and the fin pitch-to-louver pitch ratio [6].

In addition to interrupted surface concept of louvered fins, continuous fins like dimpled surfaces

have proven to effectively enhance the heat transfer capacity. The usage of dimpled surfaces has received attention due to their good heat transfer characteristics and low pressure drop penalties compared to interrupted surfaces [13].

One of the early studies was conducted by Afansayev et al. [14], where the effects of shallow dimples on flat plates on the overall heat transfer capacity and pressure drop were investigated. They reported a significant heat transfer enhancement (30-40 %) at a low pressure drop cost.

Ligrani et al. [15-16] experimentally investigated the flow structure in dimpled surfaces and showed the existence of flow recirculation zone in the upstream half of the dimple. A region of low heat transfer was observed in the upstream half of the dimple cavity followed by a high heat transfer region in the flow reattachment region in the downstream half of the dimple and the flat landing downstream of dimple [16].

Wang et al.[17], identified a symmetric 3D horseshow vortex inside a single dimple using laminar flow simulations. Line et al., Isaev and Leonte`ev, Park er al., Won and Ligrani and Park and Ligrani [18-22] investigated flow structure and heat transfer in dimpled channel in fully turbulent regimes using steady state RANS models. Patrick and Tafti [23] investigated the problem in low Reynolds numbers (Re = 50 to 2000) using DNS and LES.

In this paper a simple louvered and a dimpled-louvered fin bank geometry are investigated, both numerically and experimentally, to study the advantages of both continuous and interrupted surfaces on heat transfer augmentation and flow efficiency. Furthermore, effects of perforations on the overall flow and heat transfer characteristics will be discussed by applying small scale perforations on dimpled-louvers. In order to properly investigate the flow and heat transfer characteristics, LES method is used to model the low Reynolds turbulence flow. Velocity field is discussed for various Reynolds numbers to obtain flow efficiency and investigate the effects on heat transfer augmentation. The experimental set up shows how much increase in heat transfer will occur employing dimpled-louvered and perforated dimpled-louvered fin banks.

F_d^*

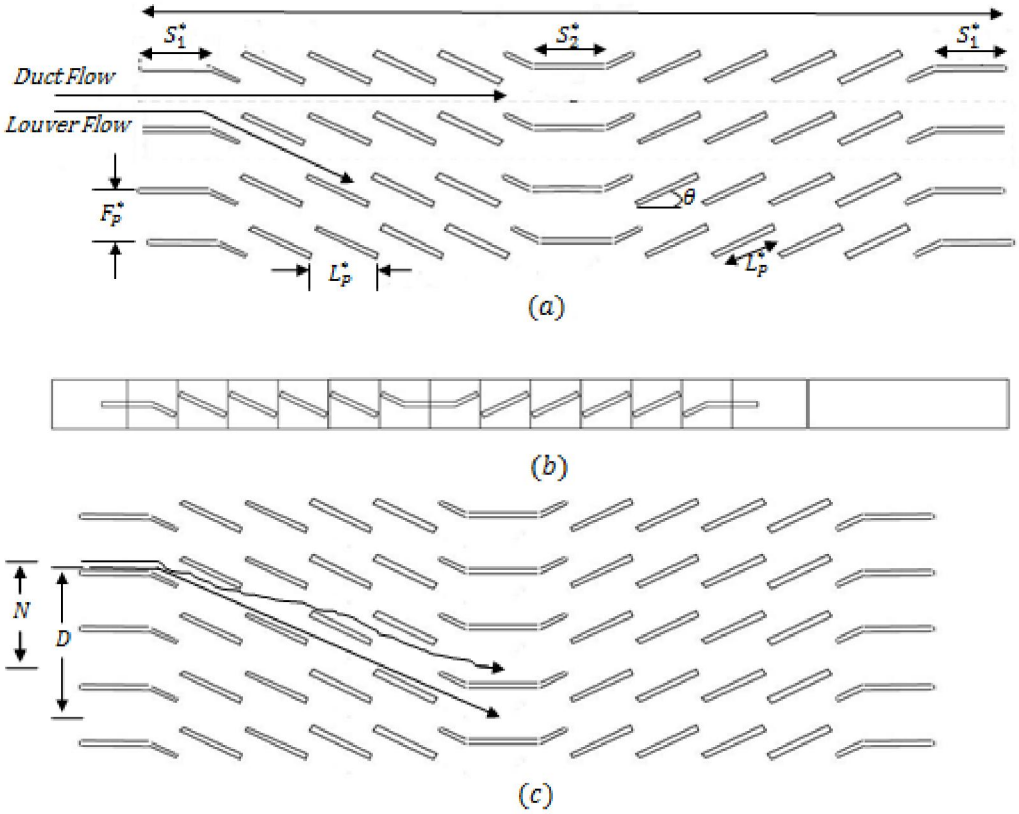

Fig.1 (a) Multilouvered fin geometry; (b) numerical analysis domain; (c) definition of experimental flow efficiency as $\eta = N/D$

Computational details:

The governing equations for momentum and energy conservation are solved in a general boundary conforming coordinate system. Fig. 1(a) shows the several rows of a multilouvered fin array while Fig. 1(b) shows the computational unit consists of only one row of louvers. Periodic boundary conditions are applied in transverse direction in order to include the thermal wake effects between successive rows of fins. Dirichlet boundary condition is applied to velocity and temperature fields at the entrance of the array.

The fin array geometry used in these calculations consists of an entrance and exit louver with four louvers on either side of the redirection louver. For all the calculations in this article, louver thickness (b) is fixed at $= 0.1$. Further geometrical details are listed in Table 1.

Table 1. List of non-dimensional geometrical parameters

Case	F_P	θ	S_1	S_2	r	d
Simple Louver	1.0	30	1.0	1.0	--	--
Dimpled Louver	1.0	30	1.0	1.0	0.2	--
Perforated Louver	1.0	30	1.0	1.0	0.2	0.25

Dimple and protrusion geometries are shown in Fig. 2. This fin geometry consists of parallel fins with line dimples and protrusions on opposite walls. Fig. 2(d) shows perforated dimple geometry layout while Fig. 2(e) shows a top view of a perforated dimple.

In this article the governing equations are non-dimensionalized by a characteristic length, the louver pitch L_P^*, a characteristic velocity, the inlet velocity to the array of fins u_{in}^* and a temperature scale given by $(T_f^* - T_{in}^*)$, where T_f^* is the louver surface temperature. No slip and no penetration conditions for the velocity field and no temperature jump for temperature field are applied on the louvers surfaces. The non-dimensionalization would result in a Reynolds number defined by $Re = Re_{in} = u_{in}^* L_p^* / \upsilon$ and Dirichlet boundary condition $u_{in} = 1$ and $T_{in} = 0$ at the entrance of the array. The Prandtl number is fixed at 0.7 for air. Patrick and Tafti [23] suggested that LES method can be used to study the low Reynolds turbulence flows in multilouvered geometries. DeJong and Jacobi [24] suggested that for similar multilouvered array layout for low Reynolds numbers the flow is steady and laminar. As the Reynolds number is increased to approximately 500, small-scale periodic transverse velocity functions generated upstream propagate downstream and louvers downstream of the redirection louver start to shed small spanwise vortices. Higher Reynolds flow leads to larger vortices and changes the flow from laminar to transition and turbulent regimes.

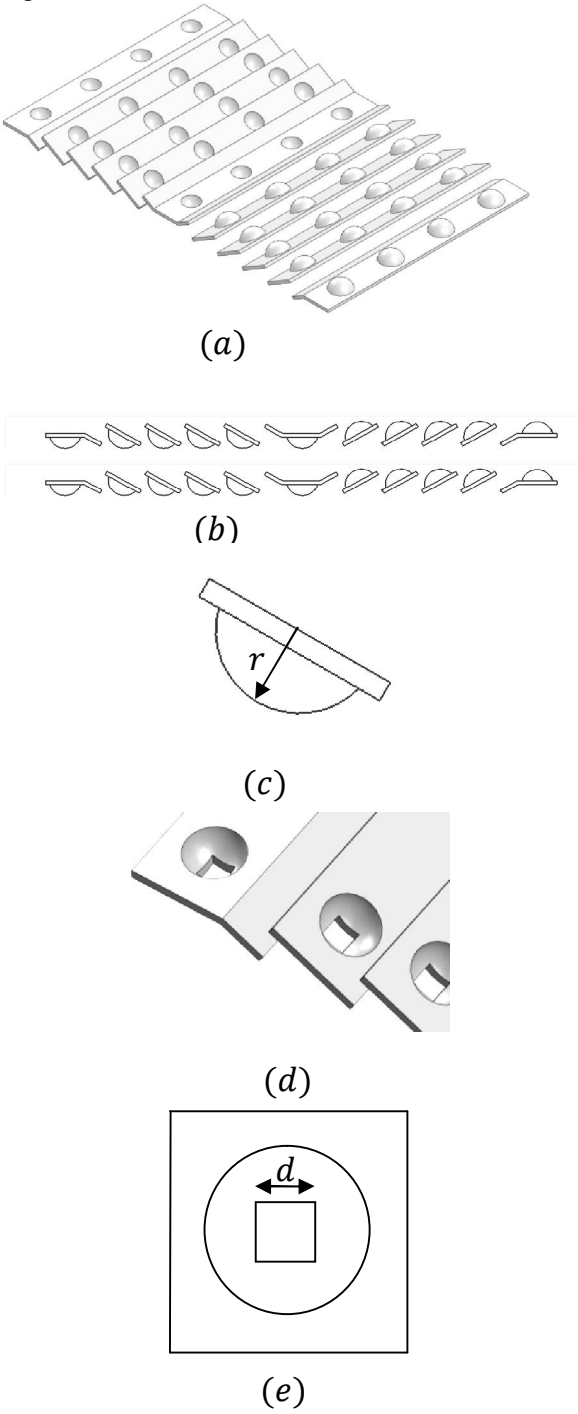

Fig.2. (a) Dimpled multilouvered fin array; (b) horizontal view of dimpled multilouvered fin array; (c) an individual dimpled louver; (d) perforated dimpled louver layout; (e) top view of a perforated dimple

We have studied low and medium Reynolds regimes (up to Re = 1000) with laminar and LES methods and came to the conclusion that in these flows laminar and LES results are in close proximity of each other. Therefore the LES method is used in low and medium Reynolds regimes in this article.

Characterization of heat transfer

It is best to describe the relationship between dimensional and non-dimensional parameters used to study the heat transfer. The dimensional heat flux on the louver surface is defined as

$$q^* = -k\frac{\partial T^*}{\partial n^*} = h^*(T_f^* - T_{ref}^*) \quad (1)$$

Where n^* is along the normal vector to the louver surface, and T_{ref}^* is the dimensional flow reference temperature. Using the non-dimensionalized variables the above equation is expressed as

$$q^* = -\frac{k}{Lp^*}\left(T_f^* - T_{in}^*\right)\frac{\partial T}{\partial n} = h^*\left(T_f^* - T_{in}^*\right)(1 - T_{ref}) \quad (2)$$

We can now define the non-dimensional heat flux and Nusselt number as

$$q = \frac{q^* Lp^*}{k\left(T_f^* - T_{in}^*\right)} = -\frac{\partial T}{\partial n} \quad (3)$$

$$Nu = \frac{h^* Lp^*}{k} = \frac{-\frac{\partial T}{\partial n}}{(1 - T_{ref})} \quad (4)$$

In this article T_{ref} is calculated by the log-mean temperature equation [6]:

$$T_{ref} = 1 - \frac{T_{out} - T_{in}}{\ln\left\{\frac{1 - T_{in}}{1 - T_{out}}\right\}} \quad (5)$$

For each louver, T_{ref} is calculated using each computational block data. T_{in} and T_{out} are averaged on the upstream and downstream boundary of each block respectively.

Flow characteristics:

As was mentioned before, the flow direction, quantified by flow efficiency, has significant implication on overall heat transfer capacity of the fin array mainly because of its strong effect on heat transfer coefficient. Flow efficiency is used to quantify the percentage of fluid flowing along the louver direction. Ranging from 0 to 1 represents complete duct directed flow to complete and ideal louvered directed flow. In experimental dye injection studies, flow efficiency is calculated as the ratio of actual transverse distance (N) traveled by the dye to the ideal distance (D) if the flow was aligned with the louver (See Fig. 1 (c))[4].

$$\eta_{exp} = \frac{N}{D} \quad (6)$$

But in numerical simulations, because the velocity field data is easily available, flow angle for flow over each louver can be obtained individually based on $\alpha = tan^{-1}(\frac{m_y}{m_x})$ where $m_y = \int v\,dx$ and $m_x = \int u\,dy$ are the average mass flow rates calculated at the top and left face of each louver. Flow efficiency is then defined as the ratio of mean flow angle which is the average flow angle throughout louvers 2-5 and 7-10 (entrance, redirection and exit louvers are excluded) to louver angle.

$$\eta = \frac{\alpha_{mean}}{\theta} \quad (1)$$

Experimental apparatus and Method

Wind Tunnel system

A low turbulence wind tunnel, Model No.TE.44/D Manufactured by PLINT and PARTNERS ENGINEERS LTD has been employed in this research. The cross section of measuring part is 460 x 460 mm and the length of the test section is 600 mm. Non-uniformity of velocity distribution is negligible. The turbulence intensity is less than 0.2 in maximum Reynolds no of our test domain. Fig 3 shows the test section of our research. Experiment apparatus is shown in Fig. 3.

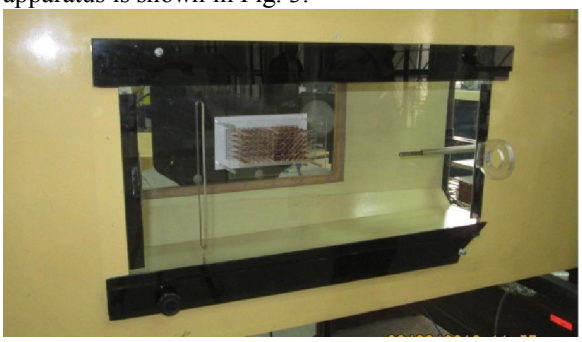

Fig.3. Experiment apparatus

Sample Models

A scales model (10:1) of inclined louvered fin banks was placed as simple model without dimples and perforations. The other two samples for simple dimples and dimple with perforations have been made with the same size. Dejoy and Jacobi presented a calculation method to find minimum required rows of fins for flow visualization studies not losing a periodic flow situation. This method is used in this research.

Flow Visualization (Smoke generation)

To visualize the flow smoke is injected at a specific point just upstream the test section. To ensure a minimal disruption of the flow and having good visibility of smoke we have generate a special Paraffin base mixture heated with special flow debi to not loose visibility in different flow velocity corresponding to different Reynolds numbers.

Some innovative methods are used to have most visible pictures of smoke path through louvers, including different color lights, filters and different photography methods.

Temperature and pressure data gathering

A temperature controller circuit is designed to maintain the temperature at 100 centigrade degree for having constant temperature condition at both ends of each louver. The controller will check the temperature 20 times a second to have minimum deviation from the set point.

A data gathering system was designed in order to have online temperature and pressure data acquisition. Then we can easily have temperature of 32 points of the louvers surfaces and easily can have 8 points for pressure reading before and after the louvers in order to find pressure drop.

An energy meter was used to count energy consumption of each sample in different Reynolds no. This device can easily inform us in which sample there is more heat transfer rate in order to fix the temperature of both sides of each louver on 100 centigrade degree.

Simulation Accuracy Verification

In order to advance forward and begin the discussions on the results of various geometries we must first verify the accuracy of the model with one of the existing sets of data. Here, we used Zhang and Tafti [6] report on the simple multilouvered geometry.

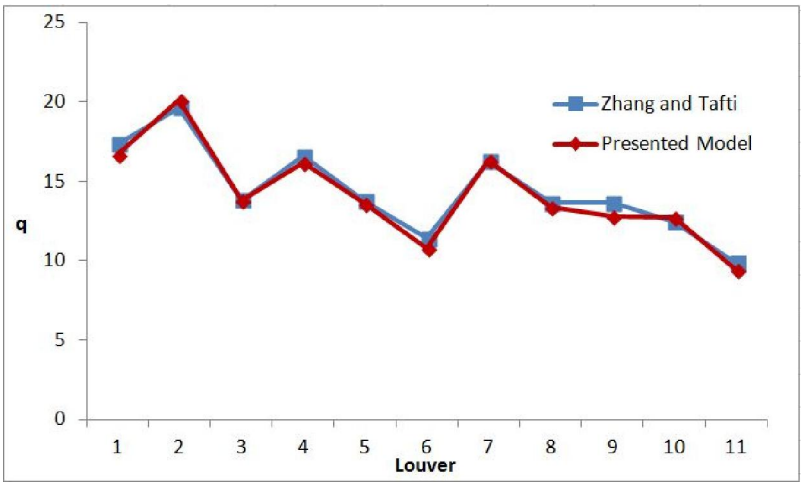

Fig. 4 Comparison of non-dimensional heat flux distribution on louver basis

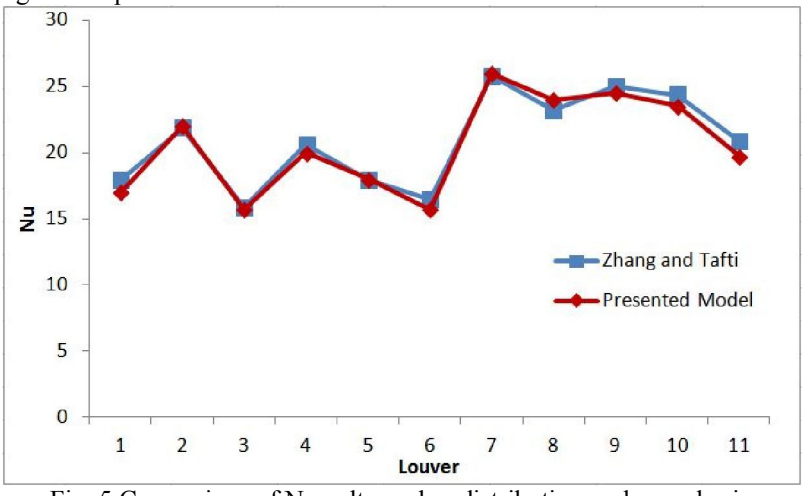

Fig. 5 Comparison of Nusselt number distribution on louver basis

Fig. 4 and Fig. 5 present the non-dimensional heat flux distribution and Nusselt number distribution, respectively, on louver basis for both Zhang and Tafti report and presented model for simple multilouvered geometry and Re = 1000. It is seen that data sets are in close proximity of each other in both figures (less than 5% deviation).

It is worth mentioning that for Re = 1000 flows the flow efficiencies reported by Zhang and Tafti [6] and the presented model differ less than 1% (Zhang and Tafti flow efficiency = 0.94, presented model flow efficiency = 0.934)

Results and Discussion

Computational

Flow and heat transfer characteristics are discussed in simple, dimpled and perforated louvered fin configurations for various Re numbers. Fig. 6 shows flow efficiencies for these geometries. It is shown that the flow efficiency increases for dimpled and perforated geometries in comparison with simple louvered geometry for the same Re numbers. Low pressure wake following each protrusion in dimpled geometry may result in favorable pressure gradient that would increase the flow efficiency. In perforated case, the favorable pressure gradient described above combined with the drain flow of the hole would further increase the flow efficiency.

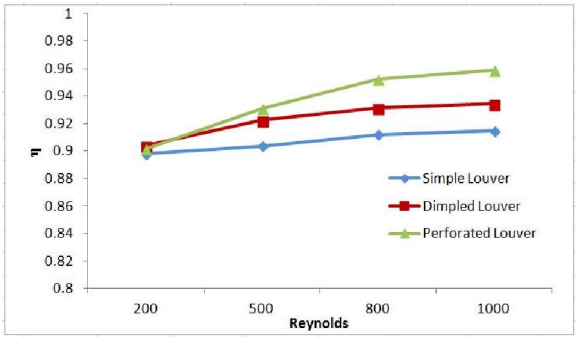

Fig. 6.Flow efficiency

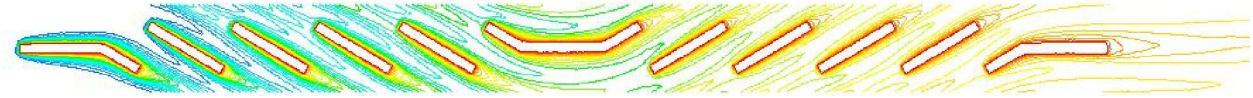

(a) Simple Louver, Re = 1000

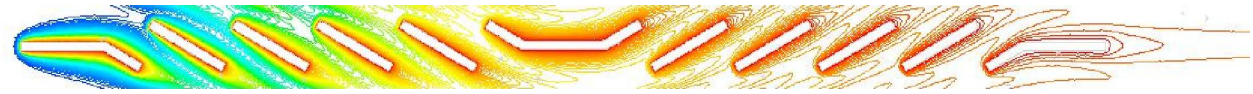

(b) Simple Louver, Re = 200

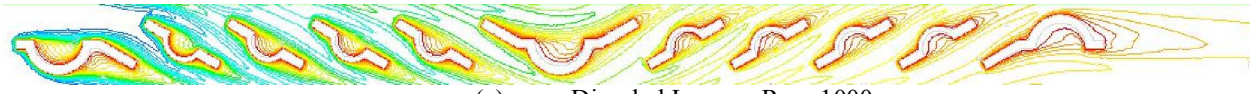

(c) Dimpled Louver, Re = 1000

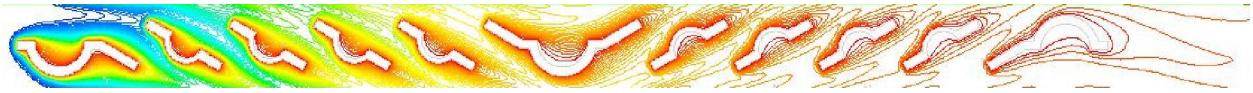

(d) Dimpled Louver, Re = 200

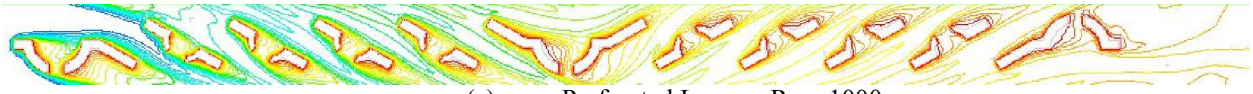

(e) Perforated Louver, Re = 1000

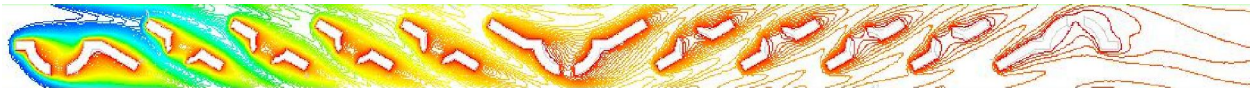

(f) Perforated Louver, Re = 200

Fig.7. Temperature contours with thermal wake effects

Tafti and Zhang [6] classified two primary mechanisms in which the louvers thermally interfere with each other, intra-fin interference and inter-fin interference. The former is dominant in duct directed flows where the thermal wakes of upstream louvers interfere with successive downstream ones. The latter is however dominant in louver directed flows where thermal wakes between fin rows interfere with each other. Intra-fin and Inter-fin thermal wake interferences can be seen in Fig. 7. It should be noted that both types of interferences occur in the same time but their dominancy is strongly dependent on flow efficiency.

Fig. 8 plots variation of non-dimensional heat flux on a louver by louver basis for three different geometries. In Fig. 8.(a), for low Re flows where the flow is less louver directed (lower flow efficiencies), the heat flux decreases continuously towards the downstream in a way that only a small portion of the total louver array heat transfer is from louvers downstream of the re-direction louver (louver number 6). This behavior is a result of thermal saturation caused by low mass flow rate (low Re) and the effects of intra-fin thermal wake interferences described above. However it should be noted that while the low Re flow efficiency is lower than the high Re flows, in this geometry, the flow is still very much louver directed ($\eta \approx 0.9$) and hence the thermal saturation effect caused by low mass flow rate is more responsible for the heat flux reduction than the intra-fin thermal wake effects (See Fig. 7). For higher Re flows, the flow is more louver directed, hence the heat flux variation is not as sharp as it is in low Re flows due to inter-fin thermal wake interferences.

Dimpled louver and perforated dimpled louver banks heat fluxes follow the above trend for simple louver geometry. Fig. 8.(b) shows that in high louver directed flows, heat fluxes of the upstream louvers are higher for perforated dimpled louvers while on the downstream of the re-direction louver the stronger inter-fin thermal wake interferences cause the heat flux to decrease. In the low Re flows however the thermal saturation effect is dominant and hence all three cases act similarly.

The distribution of T_{ref} for each louver is plotted in Fig. 9 for various cases. The reference temperature is calculated in the calculation block surrounding each louver. T_{ref} curves are dependent on flow efficiency. Fig. 9(a) shows that for high flow efficiencies, T_{ref} increase is approximately linear as the flow reaches the downstream of the array. On the other hand, for low flow efficiencies, T_{ref} increases rapidly in the upstream louvers and then increases more gradually on the downstream louvers and leaves the louver bank at a near asymptotic value. The rapid increase of T_{ref} in low Re flows leads to thermal saturation and heat flux reduction discussed above.

Nusselt number variation on a louver by louver basis is presented in Fig. 10. In perforated louver case, for Re = 1000, louver average Nu values are mostly higher than those of the simple louver case even when the louver has equal or lower heat flux in perforated case compared with the simple case, e.g. louvers 3, 7 and 9. Recalling equation (5), this is the result of higher T_{ref} in perforated case (See Fig. 9.b). The entrapped flow in the dimple cavity increases the fluid temperature and the drain flow mixture with the passing flow leads to higher reference temperature hence the higher heat transfer coefficient.

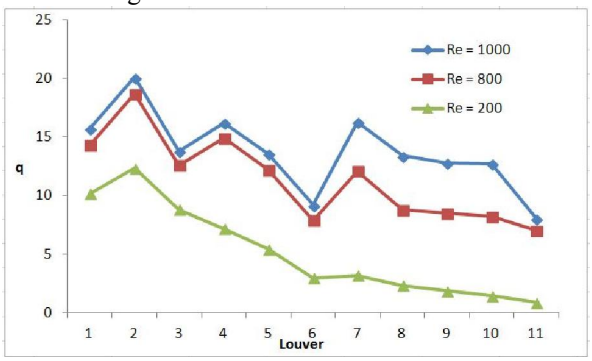

(a) Simple Louver

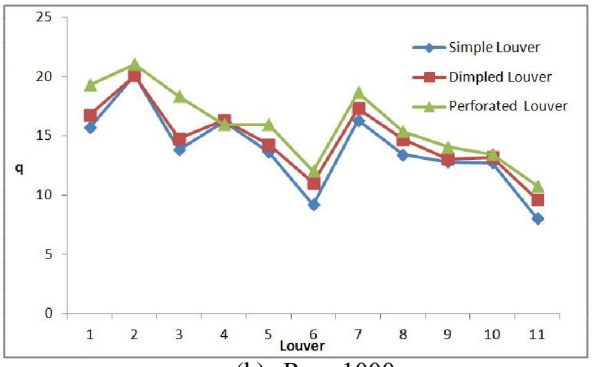

(b) Re = 1000

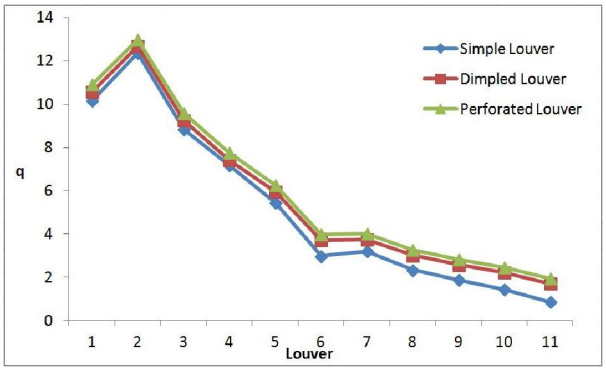

(c) Re = 200

Fig.8. Distribution of non-dimensional heat flux

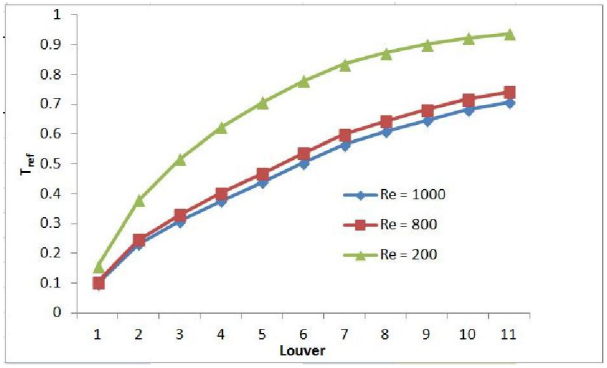

(a) Simple Louver

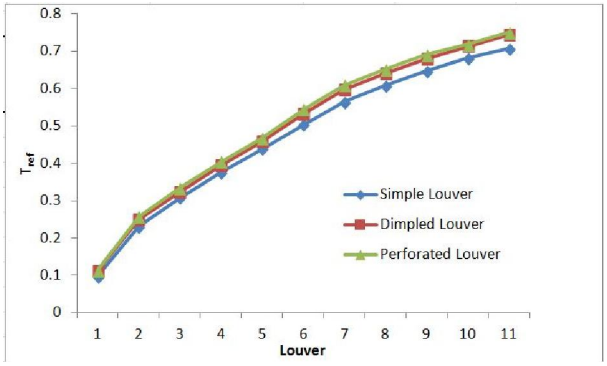

(b) Re = 1000

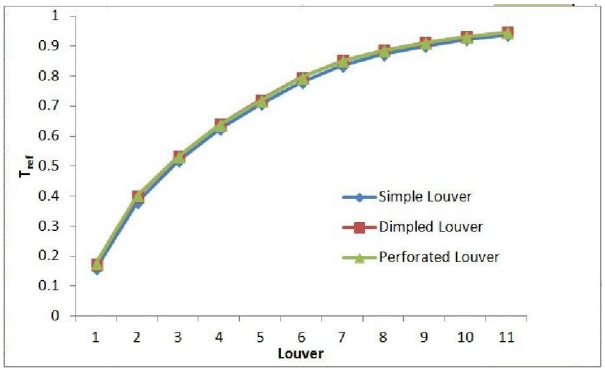

(c) Re = 200

Fig. 9 Distribution of T_{ref}

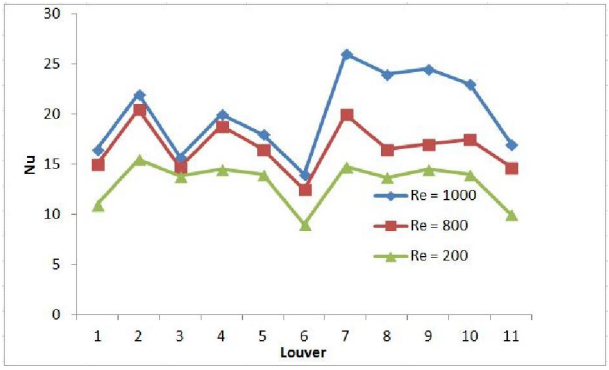

(a) Simple Louver

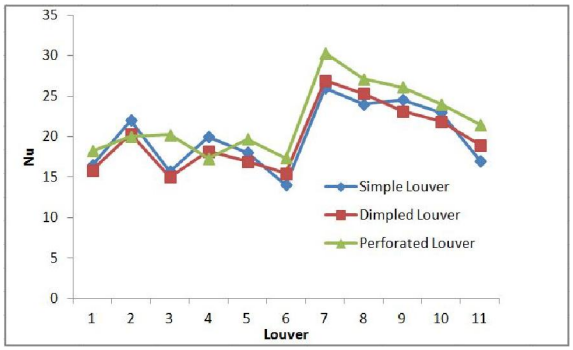

(b) Re = 1000

Fig. 10. Distribution of Nusselt

Experimental results:

Fig. 11 shows the result of visual flow efficiency for different cases for Re=1000.

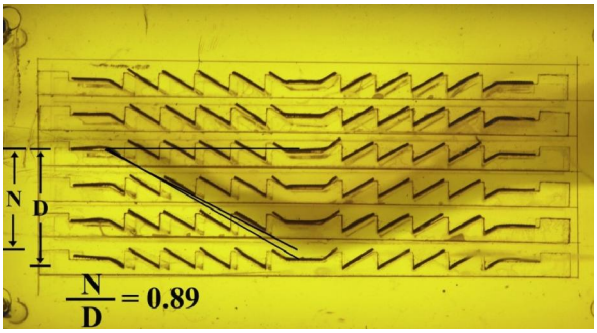

(a) Simple Louver

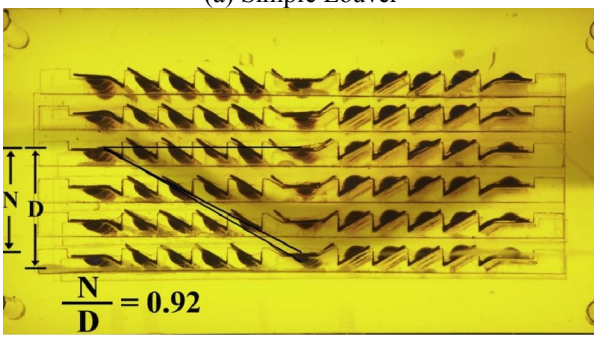

(b) Dimpled Louver

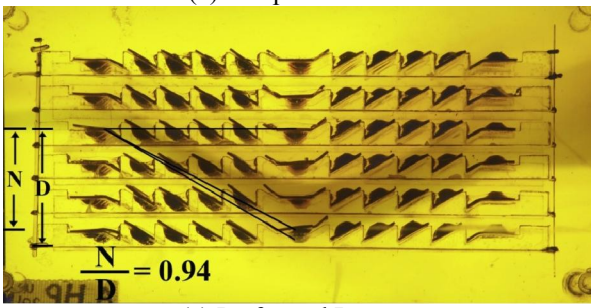

(c) Perforated Louver

Fig. 11. Experimental flow efficiency

Fig. 12(a) presents the experimental flow efficiencies for various Re numbers for three cases. The overall trend of these data is similar to those of Fig. 6. Figures 12(b) to 12(d) compare the results of visual test flow efficiencies with numerical results. As it can be seen clearly the result has completely the same trend with maximum about 5% deviation from the numerical result in different Reynolds number.

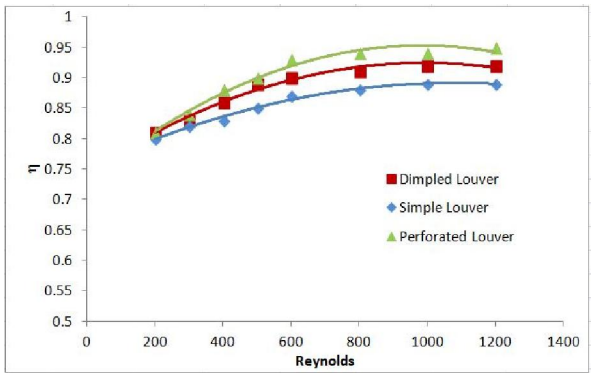

(a) Experimental flow efficiency results

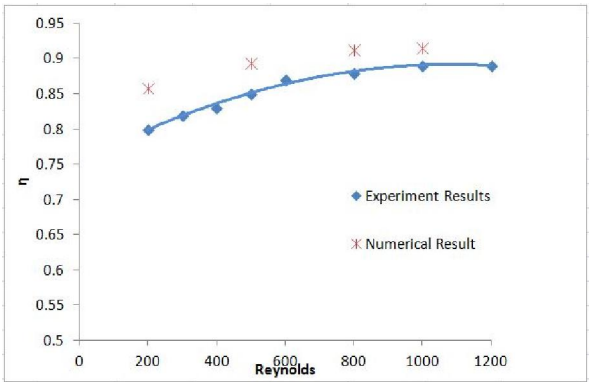

(b) Experimental and numerical flow efficiency comparison – Simple Louver

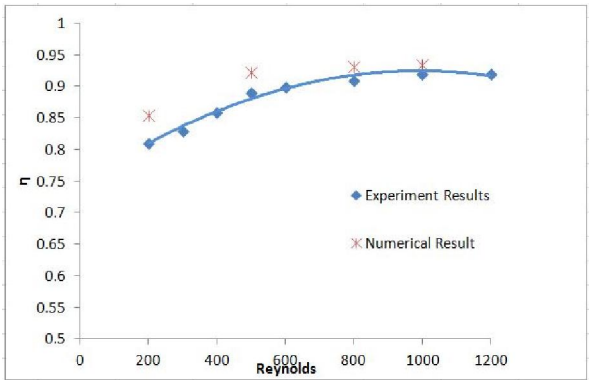

(c) Experimental and numerical flow efficiency comparison – Dimpled Louver

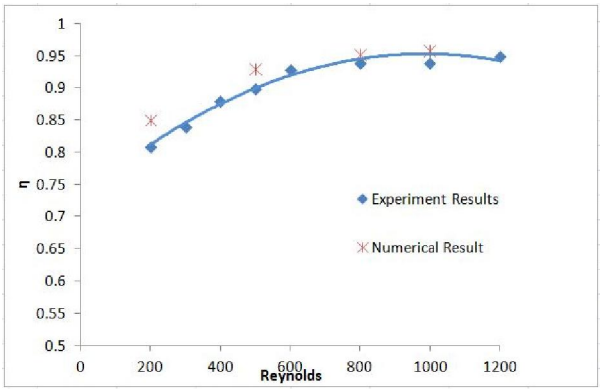

(d) Experimental and numerical flow efficiency comparison – Perforated Louver

Fig. 12. Experimental flow efficiency results and comparison with numerical results

Fig. 13 presents the total heat transfer energy ratio for dimple and dimple-perforated samples to simple louver case, calculated by the energy meter for different Reynolds numbers.

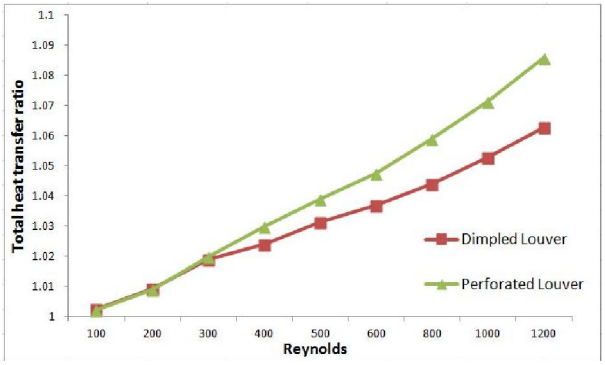

Fig. 13. Total heat transfer ratio to simple louver case

According to our expectation from numerical results for flow efficiency the total heat transfer for perforated and dimpled cases are nearly the same with simple case in low Re flows but would increase to about 6% and 9% higher than the simple case in higher Re numbers, for dimpled and perforated cases respectively. This trend was expected due to numerical results of figures 6, 8 and 10.

Conclusion

A wide range of numerical and experimental evaluations have been done for three cases, simple louver fin bank, dimple louver fin bank and dimple-perforated fin bank.

Both numerical and experimental results show that dimple-perforation sets increased the flow efficiency and total heat transfer rate up to 9% in different Reynolds no.

For higher Reynolds no this effect is more considerable because of more louver directed flow while in lower Reynolds no duct directed flow decreased this effect.

With optimizing the shape and number of dimples on each louver more heat transfer enhancement can be expected that can lead to lower total weight and material consumption of compact heat exchangers.

Nomenclature

B fin thickness
FP non-dimensional fin pitch (F_P^*/L_P^*)
Fd non-dimensional flow depth
K thermal conductivity
LP* dimensional louver pitch (characteristic length scale)
Nu Nusselt number
Q non-dimensional heat flux
Re Reynolds number
S_1, S_2 non-dimensional entrance / exit and redirection louver dimensions
R non-dimensional dimple radius
D non-dimensional hole size
T Temperature
u, v non-dimensional velocity vector components
u_{in}^* dimensional inlet velocity (characteristic velocity scale)
H heat transfer coefficient

Greek Symbols

A flow angle
Θ louver angle
N kinematic viscosity

Superscripts

* dimensional quantities

Subscripts

f, fin based on fin
In based on inlet
Louv based on louver
Out based on outlet
Ref based on reference value

References

1. Y. Chang, C. Wang, A generalized heat transfer correlation for louver fin geometry, International Journal of Heat and Mass Transfer, Vol. 40, No. 3, pp.533-544, 1997.
2. F.N. Beauvais, An aerodynamic look at automobile radiators, SAE. Paper N0. 65070, 1965.
3. C. J. Davenport, Heat transfer and fluid flow in louvered triangular ducts, Ph.D. thesis. CNAA, Lanchester Polytechnic, 1980.
4. X. Zhang, D. K. Tafti, Flow efficiency in multi-louvered fins, ACRC Paper No. ACRC TR-197, 2002.
5. R. L. Webb, P.Trauger, Flow structure in the louvered fun heat exchanger geometry, Experimental Thermal and Fluid Science, Vol. 4, pp. 205-217, 1991.
6. X. Zhang, D. K. Tafti, Classification and effects of thermal wakes on heat transfer in multilouvered fins, International Journal of Heat and Mass transfer 44 (2001) 2461-2473
7. Z. Xiaogang, D. K. Tafti, Effects of fin pitch on flow and heat transfer in multilouvered fins, ACRC Paper No. ACRC TR-150, 1999.
8. A. Achaichia, M. R. Heikal, Y. Sulaiman, and T. A. Cowell, Numerical investigation of flow and friction in louver fin arrays, 10th International Heat Transfer Conf., Heat Transfer 1994, Vol. 4, pp. 333-338, 1994.
9. L. W. Zhang, D. K. Tafti, F. M. Najjar, and S. Balachandar, Computations of flow and heat transfer in parallel-plate fin heat exchangers on the CM-5: Effects of flow unsteadiness and three-dimensionality, International Journal of Heat and Mass Transfer, Vol. 40, pp. 1325-1341, 1997.
10. L. W. Zhang, S. Balachandar, D. K. Tafti, and F. M. Najjar, Heat transfer enhancement mechanisms in inline and staggered parallel-plate fin heat exchangers, International Journal of Heat and Mass Transfer, Vol. 40, No. 10, pp. 2307-2325, 1997.
11. D. K. Tafti, L. W. Zhang, G. Wang, Time-dependent calculation procedure for fully developed and developing flow and heat transfer in louvered fin geometries, Numer. Heat Transfer, Part A 35 (1999) 225-249.
12. D. K. Tafti, G. Wang, W. Lin, Flow transition in a multilouvered fin array, International Journal of Heat and Mass Transfer 43 (2000) 901-919.
13. Mohammad A. Elyyan, Heat transfer augmentation surface using modified dimples/protrusions, Ph.D Thesis, Virginia Polytechnic Institute and State University, 2008.
14. V. N. Afansayev, Ya. P. Chudnovsky, A. I. Leontiev, and P. S. Roganov, Turbulent flow friction and heat transfer characteristics for spherical cavities on a flat plate, Experimental Thermal and Fluid Science, No. 7, pp. 1-8, 1993.
15. P. M. Ligrani, J. L. Harrison, G. I. Mahmood, and M. L. Hill, Flow structure due to dimple depressions on a channel surface, Physics of fluids, Vol. 13, No. 11, pp. 3442-3451, 2001.

16. P. M. Ligrani, N. Burgess, and S. Won, Nusselt numbers and flow structure on and above a shallow dimpled surface within a channel including effects of inlet turbulence intensity level, Journal of Turbomachinery, Vol. 127, pp. 321-330, 2005.
17. Z. Whang, K. Z. Yeo, and B. C. Khoo, numerical simulation of laminar channel flow over dimpled surface, AIAA Paper No. AIAA 2003-3964, 2003.
18. Y. L. Lin, T, I-P. Shih, and M. K. Chyu, Computations of flow and heat transfer in a channel wih rows of hemispherical cavities, ASME Paper No. 99-GT-263.
19. S. A. Isaev, A. I. Leont`ev, Numerical simulations of vortex enhancement of heat transfer under conditions of turbulent flow past a spherical dimple on the wall of a narrow channel, High Temperature 41 (5) (2003) 655-679.
20. J. Park, P. R. Desam, and P. M. Ligrani, Numerical predictions of flow structure above a dimpled surface in a channel, Numerical Heat Transfer A 45 (1) (2004) 1-20.
21. S. Won, P. M. Ligrani, Numerical predictions of flow structures and local Nusselt number ratios along and above dimpled surfaces with different dimple depths in a channel, Numerical Heat Transfer A 46 (6) (2004) 549-570.
22. J. Park, P. M. Ligrani, Numerical predictions of heat transfer and fluid flow characteristics for seven different dimpled surfaces in a channel, Numerical Heat Transfer A 47 (3) (2005) 209-232.
23. W. V. Patrick, D. K. Tafti, Computations of flow structures and heat transfer in a dimpled channel at low to moderate Reynolds numbers, ASME Paper No. HT-FED2004-56171.
24. N. C. DeJong, A. M. Jacobi, Localized flow and heat transfer interactions in louvered-fin arrays, International Journal of Heat and Mass Transfer 43 (2003) 443-455.
25. N. C. DeJong, A. M. Jacobi, Flow, heat transfer and pressure drop in the near-wall region of louvered-fin arrays, Exp. Thermal Fluid Science, Vol. 27, pp. 237-250, 2003.

7/8/2013